Compensation of an Input-Dependent Hydraulic Input Delay for a Cascaded Microfluidic Process Governed by Zweifach-Fung Effect

Delphine Bresch-Pietri[1], Nikolaos Bekiaris-Liberis[2], and Nicolas Petit[1]

***Abstract*— In this paper, we consider the control problem of a microfluidic process designed for the separation operations of a fluid containing particles in suspension, such as blood. We consider the case of several cascaded bifurcations, traveled by the fluid, to maximize the fractionation capabilities of the device for instance. We control the ratio of the flowrates in each branch, affecting the fractionation nonlinearly, through the Zweifach-Fung effect. This process can be modeled as a cascaded nonlinear dynamics, subject to input-dependent input delays of hydraulic type, corresponding to the transportation time along the branches. In this paper, we generalize our previous design for a single-bifurcation system, based on input-delay compensation, and establish sufficient conditions for input-delay compensation and exponential stabilization.**

I. Introduction

In the fields of process or biological engineering, microfluidic systems are frequently employed for their ability to handle small volumes with very high precision. These microsystems typically comprise intricate networks of channels, ranging in diameter from a few tens to a few hundred of micrometers [11], [16]. The complex geometries of these channels give rise to a variety of fluidic mechanisms. One such phenomenon, which has received considerable attention in the field of microfluidics, is the so-called Zweifach-Fung effect [6]: when a fluid carrying particles in suspension reaches a bifurcation, the volume fraction in particles increases in the high flowrate branch. Many separation devices capitalize on this phenomenon, to enrich or filter a fluid containing particles in suspension, such as blood.

This paper focuses on such a separation process governed by the Zweifach-Fung effect, featuring a simple geometry depicted in Fig 1. We consider a main channel, used to inject the fluid of interest, reaching a first bifurcation with two geometrically identical daughter channels. To enhance the fractionation capabilities of the device, the lower daughter channel further bifurcates into two identical channels. The outlets of each final branch are connected to three reservoirs: two waste reservoirs and a primary reservoir, aimed at collecting the enriched outlet fluid. Flowrates in the daughter and grand-daughter channels can be adjusted to control the volume fractions in the output reservoirs.

[1] Delphine Bresch-Pietri and Nicolas Petit are with Centre Automatique et Systèmes (CAS), Mines Paris, Université PSL, 75006 Paris, France. Email: delphine.bresch-pietri@minesparis.psl.eu

[2] Nikolaos Bekiaris-Liberis is with the Department of Electrical and Computer Engineering, Technical University of Crete, Chania, 73100, Greece. Co-funded by the European Union (ERC, C-NORA, 101088147). Views and opinions expressed are however those of the authors only and do not necessarily reflect those of the European Union or the European Research Council Executive Agency. Neither the European Union nor the granting authority can be held responsible for them

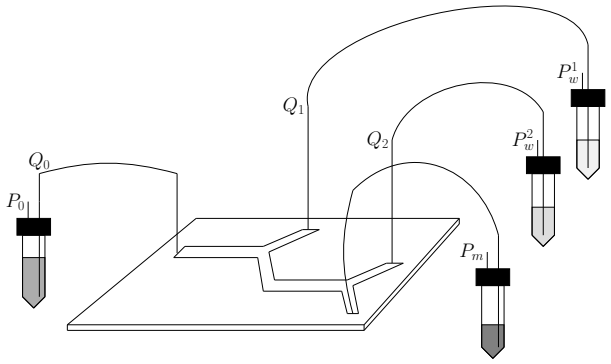

Fig. 1: Schematic view of a separation process consisting of two cascaded bifurcations, governed by the Zweifach-Fung effect. (Bifurcations at stake are Y-shaped but, alternatively, shaped bifurcations could be considered.)

Building upon the control-oriented model introduced in [13], this process can be described by a nonlinear dynamical system subject to input-dependent input delays. These delays account for the transport of particles from the bifurcation points up to the reservoirs. Assuming incompressibility of the fluid under consideration, they can be modeled as hydraulic delays [3], [5], [19], namely, delays defined implicitly through an integral of past values of the flowrates, which are here the control variables. This gives rise to a cascaded input-dependent input-delay dynamics.

In this paper, we extend our previous control design for a single-bifurcation chip from [2], which relies on *exact compensation* of the input delay, with a tailored state prediction. Prediction-based control strategies are well-established for constant delays [1], [8] and have been successfully applied in various contexts (see, for example, [7], [9], [10], [14], [15], [17]). Yet, their extension to the case of input-dependent delays revealed troublesome to achieve in general and the construction of a predictor state in [2] was only made possible due to the particular structure of the nonlinear system under consideration. This explicit prediction design reveals to be also possible for the cascaded-bifurcations system with two inputs under consideration in this paper. Owing to the cascaded structure of the plant, we propose to (i) first, use the nominal prediction-based control law from [2] to control the volume fraction in the first reservoir with the first input and (ii) then, in turns, to compensate for the delayed effect of the first input signal in the second reservoir with the second input. We formally prove that exponential regulation

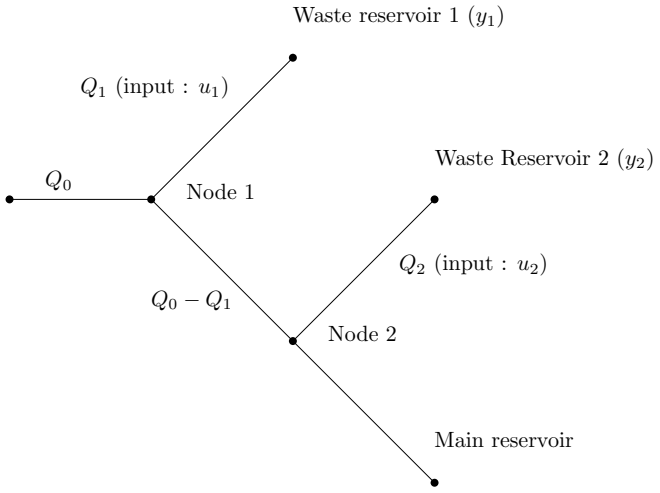

Fig. 2: Schematic view of the cascaded channels of the separation process.

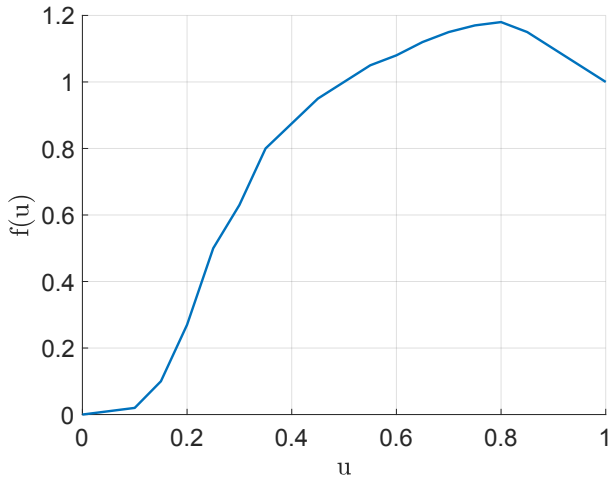

Fig. 3: Example of a possible mapping f, corresponding to the experimental data presented in [18] and reported in [13].

is achieved, under sufficient conditions bearing on the initial conditions of the plant.

The paper is organized as follows. We first formulate the problem under consideration and detail the modeling of the process at stake in Section II. The proposed control strategy is then presented in Section III, which also contains our main stabilization result, proven in Section IV. Simulation results are then reported in Section V to illustrate the merits of the proposed control design. Finally, we conclude with perspectives of future works.

II. Problem under consideration

Let us consider the microfluidic chip depicted in Fig. 1. The liquid traveling across the device consists of a solvent and particles. The overall objective of the device is to increase the volume fraction of the outlet fluid, collected in the main reservoir. This is achieved by a separation process, occuring at each node of the microfluidic chip.

Denote Q_0, Q_1 and Q_2 the (volume) flowrates in the input, daughter and grand-daughter channels, as depicted in Fig. 2. The waste reservoirs are pressurized with a high level of accuracy, allowing one to control directly the flowrates Q_1 and Q_2, due the incompressibility of the fluid under consideration. Consequently, we consider as control variables the ratios

$$u_1 = \frac{Q_1}{Q_0} \text{ and } u_2 = \frac{Q_2}{Q_0 - Q_1}\,, \tag{1}$$

which are the flowrate ratios at each node of the device. We consider the inlet flowrate Q_0 and the inlet particles volume fraction c as constant, in the following.

A. Volume of particles and hydraulic delays

When the flowrates are changed, the volume fractions right after the separation points (Nodes 1 and 2) are altered according to the flowrate ratio, in a nonlinear manner. This nonlinear mapping can be obtained from experimental measurements, and is depicted in Fig. 3. It captures the so-called Zweifach-Fung effect which, for branches of comparable geometrical characteristics, but receiving different flowrates, roughly implies that the volume fraction in particles increases in the high flowrate branch.

Let us denote v_1 and v_2 the volumes of particles inside each of the waste reservoirs. Then, v_1 satisfies

$$\dot{v}_1 = c_{Node1,1}(r_{11}(t))Q_0 u_1(t)\,, \tag{2}$$

in which, according to the Zweifach-Fung effect, the particle ratio in the upper branch right after Node 1 is

$$c_{Node1,1}(t) = cf(u_1(t))\,, \tag{3}$$

and where $r_{11}(t) = t - \delta_{11}(t)$ is a delay term, capturing the transport time from Node 1 to Reservoir 1. In details, this dynamics accounts for (i) the nonlinear separation phenomenon occurring right after Node 1, in (3); (ii) the transport time of the particle fraction along the upper daughter branch, and (iii) the incompressibility of the flow, leading to a spatially uniform flow rate along the branch, and thus, to the appearance of $u_1(t)$ in (2). The incompressibility of the flow (plug-flow assumption, see [12]) also leads to the following implicit characterization of the hydraulic delay (see [4])

$$\int_{r_{11}(t)}^{t} u_1(s)ds = \frac{V_{11}}{Q_0} \triangleq T_{11}\,, \quad t \geq 0\,, \tag{4}$$

in which V_{11} is the volume of the first channel.

Similarly, the volume of particles in the second reservoir satisfies

$$\dot{v}_2 = c_{Node2,1}(r_{21}(t))(Q_0 - Q_1(t))u_2(t) \tag{5}$$

in which, similarly, due to the Zweifach-Fung effect and transport phenomena,

$$c_{Node2,1}(t) = c_{Node1,2}(r_{12}(t))f(u_2(t)) \tag{6}$$

$$c_{Node1,2}(t) = cf(1 - u_1(t)) \triangleq cg(u_1(t)) \tag{7}$$

where r_{12} and r_{21} are the delay fonctions corresponding to the transport times, respectively, from Node 1 to Node 2 and

from Node 2 to Reservoir 2. They are defined as the (unique) solutions to

$$\int_{r_{12}(t)}^{t}(1-u_1(s))ds = \frac{V_{12}}{Q_0} \triangleq T_{12}\,, \quad t \geq 0 \tag{8}$$

$$\int_{r_{21}(t)}^{t}u_2(s)(1-u_1(s))ds = \frac{V_{21}}{Q_0} \triangleq T_{21}\,, \quad t \geq 0 \tag{9}$$

in which V_{12} and V_{21} are the volumes of the corresponding branches.

For the delay functions to be well-defined through (4), (8), and (9), the flowrates, and thus, the inputs u_1 and u_2, are assumed to be lower bounded by a positive constant (see [4]).

B. Volume fraction dynamics

Let us now define the outputs of interest, which are the ratios of volume fractions in the first and second reservoirs[1], respectively,

$$y_1(t) = \frac{v_1(t)}{cQ_0w_1(t)} \text{ and } y_2(t) = \frac{v_2(t)}{cQ_0w_2(t)}\,, \tag{10}$$

in which w_1 and w_2 are the (normalized) volumes of fluid in the two reservoirs. Gathering (2)–(9), it follows that

$$\dot{y}_1(t) = \frac{u_1(t)}{w_1(t)}\left(f(u_1(r_{11}(t))) - y_1(t)\right)\,, \tag{11}$$

$$\dot{w}_1(t) = u_1(t)\,, \tag{12}$$

$$\dot{y}_2(t) = \frac{u_2(t)(1-u_1(t))}{w_2(t)} \times \left(f(u_2(r_{21}(t)))g(u_1(r_{12}\circ r_{21}(t))) - y_2(t)\right)\,, \tag{13}$$

$$\dot{w}_2(t) = u_2(t)(1-u_1(t))\,, \tag{14}$$

in which the delays r_{11}, r_{12} and r_{21} are defined through (4) and (8)–(9), f is assumed to satisfy the following property, and $g(u) = f(1-u)$.

Assumption 1: The function $f : [\underline{u}, \overline{u}] \mapsto \mathbb{R}_+^\star$ (with $0 < \underline{u} < \overline{u} < 1$) is Lipschitz with constant L_f, increasing, and its corresponding inverse is Lipschitz with constant $L_{f^{-1}}$.

III. Control design

The control objective is to regulate the ratios y_1, y_2 of volume fractions in the waste reservoirs to reference values y_1^r, y_2^r (and thus, correspondingly, the one in the main reservoir, by conservation law). Assuming the references are achievable, that is, $(y_1^r, y_2^r) \in [f(\underline{u}), f(\overline{u})] \times [f(\underline{u})^2, f(\overline{u})^2]$, we denote $u_1^r = f^{-1}(y_1^r)$ and $u_2^r = f^{-1}\left(\frac{y_2^r}{g(u_1^r)}\right)$ the corresponding reference inputs.

Let us first observe that the dynamics (11) and (13) of the ratios of volume fractions are asymptotically stable in open-loop (as formally proven in Lemma 1 in [2] for a single-bifurcation device). Yet, due to their large open-loop response time, we wish to design a closed-loop strategy. In the sequel, following [2], we design a predictor-based feedback law.

[1]The one in the main reservoir, which is the main variable of interest, can then indirectly be controlled.

A. Predictors

To formulate exact predictors for the system states, we follow the design strategy of [2]. First, using the variation of constant formula for (11) between t and $r_{11}^{-1}(t)$, the dynamics (12) and the properties of (4) (see [2] for details), it follows that

$$y_1\left(r_{11}^{-1}(t)\right) = \exp\left(-\int_t^{r_{11}^{-1}(t)}\frac{u_1(s)}{w_1(s)}ds\right)y_1(t) \tag{15}$$

$$+\int_t^{r_{11}^{-1}(t)}\exp\left(-\int_s^{r_{11}^{-1}(t)}\frac{u_1(\xi)}{w_1(\xi)}d\xi\right)\frac{u_1(s)}{w_1(s)}f(u_1(r_{11}(s)))ds$$

$$= \frac{1}{w_1(t)+T_{11}}\left(w_1(t)y_1(t) + \int_{r_{11}(t)}^{t}u_1(s)f(u_1(s))ds\right)$$

$$\triangleq p_1(t)\,, \tag{16}$$

observing that, from (4), $w(r_{11}^{-1}(t)) = w_1(t) + T_{11}$ and performing a change of variable on the last integral in (15) . Thus, one can compute the future value of y_1 at time $r_{11}^{-1}(t)$ in a causal manner, namely, based only on (current and past) states and inputs values, available at time t.

Similarly, one obtains for the second reservoir

$$y_2\left(r_{21}^{-1}(t)\right) = \exp\left(-\int_t^{r_{21}^{-1}(t)}\frac{u_2(s)(1-u_1(s))}{w_2(s)}ds\right)y_2(t)$$

$$+\int_t^{r_{21}^{-1}(t)}\exp\left(-\int_s^{r_{21}^{-1}(t)}\frac{u_2(\xi)(1-u_1(\xi))}{w_2(\xi)}d\xi\right) \tag{17}$$

$$\times\frac{u_2(s)(1-u_1(s))}{w_2(s)}f(u_2(r_{21}(s)))g(u_1(r_{12}\circ r_{21}(s)))ds$$

$$= \frac{1}{w_2(t)+T_{21}}\Bigg(w_2(t)y_2(t) + \int_{r_{21}(t)}^{t}u_2(s)(1-u_1(s))$$

$$\times f(u_2(s))g(u_1(r_{12}(s)))ds\Bigg) \triangleq p_2(t)\,. \tag{18}$$

Again, this expression only depends on past values of the states and the inputs, available at time t, and can thus be computed.

B. Predictor-based control design

Due to the cascaded structure of the dynamics (11), (13), we propose to follow a two-steps control procedure: (i) first, we design u_1 to control solely y_1; (ii) then, in turn, we design u_2 to control y_2, according to the fixed past values of u_1 appearing in (13) (which are further delayed, as $r_{12}\circ r_{21}(t) < r_{21}(t)$).

We thus first design u_1. In virtue of (11), and due to the previous explicit predictor design, we thus pick the control law for the first reservoir such that

$$f(u_1(t)) = p_1(t) - k_1(w_1(t)+T_{11})(p_1(t) - y_1^r) \tag{19}$$

in which p_1 is the predictor of y_1 defined in (16) and $k_1 > 0$ is fixed and has to be tuned. Provided that the right-hand side of (19) takes values in $[f(\underline{u}), f(\overline{u})]$, one can then directly obtain (by Assumption 1)

$$u_1(t) = f^{-1}\left(p_1(t) - k_1(w_1(t)+T_{11})(p_1(t) - y_1^r)\right) \tag{20}$$

Observe that this control law is the same as the one obtained in the single-bifurcation case in [2].

Similarly, the control law for the second reservoir is then chosen as

$$u_2(t) = f^{-1}\Bigg(\frac{1}{g(u_1(r_{12}(t)))}(p_2(t) - k_2(w_2(t)+T_{21})(p_2(t)-y_2^r))\Bigg), \quad (21)$$

where $k_2 > 0$ has to be tuned. The objective of these control laws is to linearize the system in closed-loop, that is, to obtain the closed-loop dynamics

$$\dot{y}_1(t) = -k_1 u_1(t)(y_1(t) - y_1^r) \quad (22)$$
$$\dot{y}_2(t) = -k_2 u_2(t)(1-u_1(t))(y_2(t) - y_2^r) \quad (23)$$

after a certain time, namely, after both of the closed-loop input signals reach the plant.

For these control laws to be well-defined, one needs to guarantee that the inverse of f is well-defined, namely that the arguments of (20) and (21) take values in $[\underline{u}, \overline{u}]$. This is the objective of our main result which we now state.

C. Main result

Theorem 1: Consider the closed-loop system consisting of the dynamics (11)–(14) satisfying Assumption 1 and subject to the input delays (4), (8)–(9), together with the control law defined through (16), (18) and (20)–(21). Denote $\Psi_i^0 = (y_i^0, w_i^0, u_i^0)$ $(i = 1, 2)$, $\Psi^0 = (\Psi_1^0, \Psi_2^0)$, $P_1(\Psi_1^0) = p_1(0)$ and $P_2(\Psi^0) = p_2(0)$, with p_1, p_2 defined in (16), (18), and define

$$F_m(\Psi_1^0, y_1^r) = (g(f^{-1}(y_1^r)) + L_f H(\Psi_1^0, y_1^r)) f(\underline{u}), \quad (24)$$
$$F_M(\Psi_1^0, y_1^r) = (g(f^{-1}(y_1^r)) - L_f H(\Psi_1^0, y_1^r)) f(\overline{u}), \quad (25)$$
$$H(\Psi_1^0, y_1^r) = \max\Bigg\{ \sup_{t\in[r_{12}(0),0)} |u_1^0(t) - f^{-1}(y_1^r)|, L_{f^{-1}} W(e^{-1}) |P_1(\Psi_1^0) - y_1^r| \Bigg\}, \quad (26)$$

in which W is the Lambert function. Then, for all initial conditions $y_1^0 \in [f(\underline{u}), f(\overline{u})], y_2^0 \in [f(\underline{u})^2, f(\overline{u})^2]$, $w_1^0 > 0$, $w_2^0 > 0$, $u_1^0 \in C([\min\{r_{11}(0), r_{12} \circ r_{21}(0)\}, 0], [\underline{u}, \overline{u}])$ and $u_2^0 \in C([r_{21}(0), 0], [\underline{u}, \overline{u}])$ such that

$$H(\Psi_1^0, y_1^r) < \frac{f(\overline{u}) - f(\underline{u})}{f(\overline{u}) + f(\underline{u})} \frac{g(f^{-1}(y_1^r))}{L_f}, \quad (27)$$
$$y_1^r - f(\overline{u}) \le (P_1(\Psi_1^0) - y_1^r) e^{-1-W(e^{-1})} \le y_1^r - f(\underline{u}), \quad (28)$$
$$e^2 F_m(\Psi_1^0, y_1^r) \le (1+e^2) y_2^r - P_2(\Psi^0) \le e^2 F_M(\Psi_1^0, y_1^r), \quad (29)$$

there exist $k_1, k_2 > 0$ such that exponential regulation is achieved, namely,

$$|y(t) - y^r| \le |y(\sigma(0)) - y^r| \times e^{-\min\{k_1,k_2\}\underline{u}(1-\overline{u})(t-\sigma(0))}, \quad t \ge \sigma(0), \quad (30)$$
$$(u_1(t), u_2(t)) \in [\underline{u}, \overline{u}]^2, \quad t \ge 0, \quad (31)$$

with $\sigma(0) = \max\{r_{11}^{-1}(0), r_{21}^{-1}(0)\}$.

As will appear in the next section, the proof of this result is constructive and proposes explicit choices for the feedback gains k_1, k_2. Yet, future works will focus on improving their tuning.

According to this result, exponential regulation can be achieved under the conditions (27)–(29). The two first conditions restrict the magnitude of the initial condition of the first reservoir and require it to be sufficiently close to the equilibrium value, that is, (27)–(28) limit the magnitude of both $|u_1^0 - u_1^r|$ and $P_1(\Psi_1^0) - y_1^r$. On the other hand, (28) bears on the initial condition of the second reservoir, limiting the magnitude of $P_2(\Psi^0) - y_2^r$ depending on the initial conditions of the first reservoir. This is consistent with the structure of the dynamics and the corresponding control design, as the first input is designed to regulate the first reservoir but also impact the second reservoir dynamics, in a somehow passive manner.

Besides, one can observe that, compared to the single bifurcation study of [2], the set of stabilizable initial conditions for the first reservoir has been reduced. This is a direct consequence of the addition of a second reservoir in the set-up. Indeed, as the dynamics of the second reservoir involves u_1, the regulation of the first reservoir may, in turn, put excessive constraints on the actuation of the second reservoir dynamics, prohibiting its regulation. This limits the set of initial conditions which can be considered.

Robustness properties of this design should of course be considered in future works, to take into account uncertain initial conditions.

IV. Proof of Theorem 1

According to the previous design elements, the proposed control law achieves closed-loop exponential stabilization if and only if there exist $k_1, k_2 > 0$ such that (31) holds. Indeed, in this case, the closed-loop system is well-defined and (22)–(23) guarantee exponential convergence, with decay rate $\min\{k_1, k_2\}\underline{u}(1-\overline{u})$.

In the sequel of the proof, we will study recursively the two control laws to guarantee this condition.

A. Condition on the first input u_1

Using the monotonicity of f and the control law (20), the part of condition (31) bearing solely on u_1 reformulates as:

$$\exists\, k_1 > 0 \quad \forall t \ge 0 \quad (32)$$
$$y_1^r + (1 - k_1(w_1(t) + T_{11}))(p_1(t) - y_1^r) \in [f(\underline{u}), f(\overline{u})].$$

This condition being independent of the second reservoir, the single-birfurcation approach of [2] can be applied. Namely, observing that, from (12) and (22),

$$w_1(t) = w_1^0 + \int_0^t u_1(s)ds, \quad (33)$$
$$p_1(t) - y_1^r = \exp\left(-k_1 \int_0^t u_1(s)ds\right)(p_1(0) - y_1^r), \quad (34)$$

the following result can be obtained from Lemma 4 in Appendix, applied with $(a,p,b,k)=(y_1^r,p_1(0),w_1^0+T_{11},k_1)$, $h=k_1\int_0^t u_1(s)ds$ (which spans $\mathbb{R}_+$ provided $k_1>0$ and $u_1\geq\underline{u}>0$), and $(G_m,G_M)=(f(\underline{u}),f(\overline{u}))$.

Lemma 1 (Corollary of Theorem 2 in [2]): Consider the closed-loop system consisting of the dynamics (11)–(12) satisfying Assumption 1 and subject to the input-delay (4), together with the control law defined through (16) and (20). Denote $\Psi_1^0=(y_1^0,w_1^0,u_1^0)$ and $P_1(\Psi_1^0)=p_1(0)$. Then, Eq. (32) holds iff (35)

$$(1+e^2)y_1^r-e^2f(\overline{u})\leq P_1(\Psi_1^0)\leq(1+e^2)y_1^r-e^2f(\underline{u})$$

and this holds for all $k_1\in(0,k^\star(f(\underline{u}),f(\overline{u}),y_1^r,P_1(\Psi_1^0),w_1^0+T_{11}))$ in which $k^\star$ is defined in (54).

B. Condition on the second input u_2

Consider now the first input u_1 as fixed, and taking values in $[\underline{u},\overline{u}]$. Using the monotonicity of f and the control law (21), the part of condition (31) bearing on u_2 reformulates as:

$$\begin{aligned}\exists\, k_2>0\ \forall t\geq 0\quad & y_2^r+(1-k_2(w_2(t)+T_{21}))(p_2(t)-y_2^r)\\ &\in[g(u_1(r_{12}(t)))f(\underline{u}),g(u_1(r_{12}(t)))f(\overline{u})]\end{aligned}\tag{36}$$

Such a condition reveals intricate to study, as it involves time-varying bounds, due to the appearance of delayed values of the first input signal. Consequently, we propose to formulate an alternative sufficient condition, involving constant interval bounds.

To modify the interval in Eq. (36), let us observe that, for $t\geq 0$,

$$g(u_1(r_{12}(t)))\leq g(u_1^r)+\sup_{t\geq r_{12}(0)}(g(u_1(t))-g(u_1^r))\tag{37}$$

$$\leq g(u_1^r)+L_f\max\left\{\sup_{t\in[r_{12}(0),0)}|u_1(t)-u_1^r|,\ \sup_{t\geq 0}|u_1(t)-u_1^r|\right\}\tag{38}$$

where we used Assumption 1. Besides, from (20), for $t\geq 0$, it holds

$$|u_1(t)-u_1^r|=\tag{39}$$

$$|f^{-1}\left(y_1^r-(1-k_1(w_1(t)+T_{11}))(p_1(t)-y_1^r)\right)-f^{-1}(y_1^r)|$$

$$\leq L_{f^{-1}}|(1-k_1(w_1(t)+T_{11}))(p_1(t)-y_1^r)|\tag{40}$$

$$\leq L_{f^{-1}}\kappa(y_1^r,P_1(\Psi_1^0),w_1^0+T_{11},k_1)\,,\tag{41}$$

in which κ is defined in (50). Similar considerations lead to

$$g(u_1(r_{12}(t)))\geq g(u_1^r)-L_f\max\left\{\sup_{t\in[r_{12}(0),0)}|u_1(t)-u_1^r|,\ L_{f^{-1}}\kappa(y_1^r,\Psi_1^0,w_1^0+T_{11},k_1)\right\}.\tag{42}$$

A sufficient condition for Eq. (36) to hold is thus

$$\exists\, k_2>0\quad\forall t\geq 0\quad y_2^r+(1-k_2(w_2(t)+T_{21}))\tag{43}$$

$$\times(p_2(t)-y_2^r)\in[F_m(\Psi_1^0,y_1^r,k_1),F_M(\Psi_1^0,y_1^r,k_1)]\,,$$

with

$$F_m(\Psi_1^0,y_1^r,k_1)=f(\underline{u})\Bigg(g(u_1^r)+L_f\max\Bigg\{\sup_{t\in[r_{12}(0),0)}|u_1(t)-u_1^r|,L_{f^{-1}}\kappa(y_1^r,P_1(\Psi_1^0),w_1^0+T_{11},k_1)\Bigg\}\Bigg)\,,\tag{44}$$

$$F_M(\Psi_1^0,y_1^r,k_1)=f(\overline{u})\Bigg(g(u_1^r)-L_f\max\Bigg\{\sup_{t\in[r_{12}(0),0)}|u_1(t)-u_1^r|,L_{f^{-1}}\kappa(y_1^r,P_1(\Psi_1^0),w_1^0+T_{11},k_1)\Bigg\}\Bigg)\,.\tag{45}$$

C. Conclusion of the proof of Theorem 1

We wish to guarantee conditions (32) and (43). With this aim in view, let us pick $k_1=\frac{1-W(e^{-1})}{w_1^0+T_{11}}>0$. Under (28), one can check that $k_1\in(0,k^\star(f(\underline{u}),f(\overline{u}),y_1^r,p_1^0,w_1^0+T_{11}))$ and thus, as (28) implies (35), from Lemma 1, (32) holds.

Besides, due to Lemma 3, $\kappa(y_1^r,P_1(\Psi_1^0),w_1^0+T_{11},k_1)$ is minimal and equal to $W(e^{-1})\,|P_1^0(\Psi_1^0)-y_1^r|$. Consequently, in virtue of (27),

$$F_m(\Psi_1^0,y_1^r,k_1)<F_M(\Psi_1^0,y_1^r,k_1)\,.\tag{46}$$

Then, from Lemma 4 in Appendix applied with $(a,p,b,k)=(y_2^r,p_2(0),w_2^0+T_{21},k_2)$, $h=k_2\int_0^t u_1(s)(1-u_1(s))ds$ (which spans $\mathbb{R}_+$ provided $k_2>0$ and $u_1,u_2\geq\underline{u}>0$) and $(G_m,G_M)=(F_m,F_M)$, it follows that (43) holds iff (29) is satisfied (and for $k_2\in(0,k^\star(F_m,F_M,y_2^r,P_2(\Psi^0),w_2^0+T_{21}))$.

To conclude the proof of Theorem 1, notice that the closed-loop dynamics (22)–(23) imply

$$y_1(t)-y_1^r=e^{-k_1\int_{r_{11}^{-1}(0)}^t u_1(s)ds}(y_1(r_{11}^{-1}(0))-y_1^r)\,,\quad\text{for } t\geq r_{11}^{-1}(0)\,,\tag{47}$$

$$y_2(t)-y_2^r=e^{-k_2\int_{r_{21}^{-1}(0)}^t u_2(s)(1-u_1(s))ds}(y_2(r_{21}^{-1}(0))-y_2^r)\,,\quad\text{for } t\geq r_{21}^{-1}\,,(0)\tag{48}$$

from which (30) then follows.

V. Simulation results

Simulations have been performed over Matlab/Simulink, to illustrate the interest of the proposed control strategy and evaluate the conservatism of the obtained stabilization conditions.

We consider the function f pictured in Fig. 3, corresponding to $L_f=4.6$, $L_{f^{-1}}=5$ and $[\underline{u},\overline{u}]=[0.01,0.8]$. The case study under consideration consists in a chip originally at the equilibrium corresponding to $y_1^0=y_2^0=0.9$, that is, with $u_1^0=f^{-1}(y_1^0)\approx 0.42$ and $u_2^0=f^{-1}\left(\frac{y_2^0}{g(u_1^0)}\right)\approx 0.38$. The corresponding delay values are $r_{11}(0)=2.4$, $r_{12}(0)\approx 1.71$ and $r_{21}(0)\approx 4.54s$.

The reference changes to $(y_1^r,y_2^r)=(0.86,0.88)$ at time $t=0.5s$. This set-up corresponds to a step of ratio of volume fraction in the main reservoir from $y_3^0\approx 1.17$ to

$y_3^r = g(u_1^r)g(u_2^r) \approx 1.21$, which illustrates the fractionation capabilities of this cascaded device (indeed, a single-bifurcation one only allows for an equilibrium in the range of f, that is, a ratio smaller than 1.18).

For these initial conditions, the conditions (27)–(28) of Theorem 1 are satisfied for values of y_1^r in the interval $[0.86, 0.94]$, while, for $y_1^r = 0.86$, condition (29) holds for values of y_2^r in the interval $[0.11, 1.15]$. This illustrates that the sufficient conditions of Theorem 1 impose restrictions on the achievable reference for the first reservoir.

We picked the feedback gain following the construction proposed in the proof, that is, $k_1 = \frac{1-W(e^{-1})}{w_1^0+T_{11}} \approx 0.71$ and $k_2 = 3 \in (0, k^\star(F_m, F_M, y_2^r, P_2(\Psi^0), w_2^0 + T_{21})) \approx (0, 44.42)$. One can observe that the proposed prediction-based control strategy does achieve exponential regulation, exactly compensating for the input-delay, as nominal delay-free exponential convergence is obtained.

Interestingly, one can observe the effect of canceling the cascade of u_1 in the second dynamics via (21) (which involves the delayed term $g(u_1(r_{12}(t)))$) on the time-evolution of u_2. Indeed, a first sudden variation can be observed when the step occurs, at time $t = 0.5$ and then, around $t = 2s$, the delayed effect of the drop of $g(u_1)$ occurring at $t = 0.5$ generates another discontinuity for u_2.

VI. Conclusion

In this paper, we have considered a cascaded microfluidic separation process, modeled as a nonlinear dynamics subject to input-dependent hydraulic input delays. Following our previous design from [2], we proposed a two-step prediction-based control design, exactly compensating for the input-delay. Besides, we provided sufficient conditions to achieve exponential regulation, characterizing the set of initial conditions of interest.

Future works will focus on characterizing more closely the feedback gains of interest, to improve closed-loop performances. Also, an alternative viewpoint could be to explicitly characterize the set of initial conditions that could be stabilized, depending on the feedback gains. This is a direction of future research, along with taking into account input saturation in the closed-loop analysis.

Besides, this study opens the path to explore many other interesting questions. For instance, one can wonder if, instead of intending to regulate the reservoirs simultaneously as considered in this paper, it may be worth sequencing them and, in that case, in which order. Other perspectives include the extension of this technique to multiple cascades and to the case of a sole common waste reservoir, leading to a single-input control problem.

Appendix: Intermediate results

In this section, we gather intermediate results which are helpful for closed-looop stability analysis.

Let us consider scalar variables a, b, p, k, with $b, k > 0$ and define the function

$$G : h \geq 0 \mapsto a + (1 - bk - h)e^{-h}(p - a) \qquad (49)$$

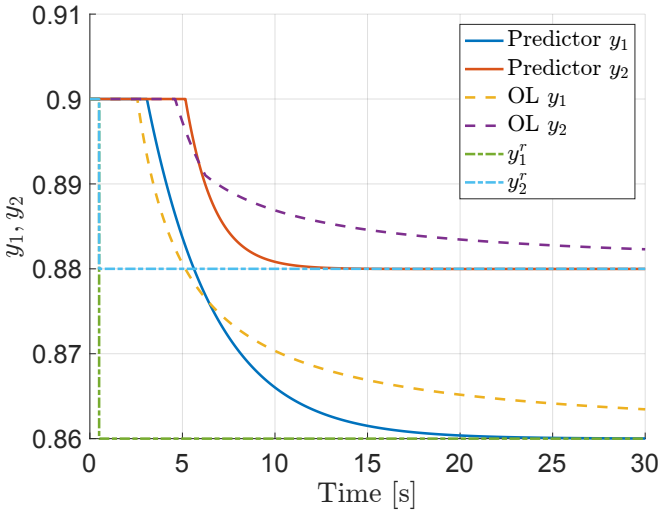

(a) Time-evolution of the ratios of volume fractions in each waste reservoir, for the proposed prediction-based control strategy and in open-loop.

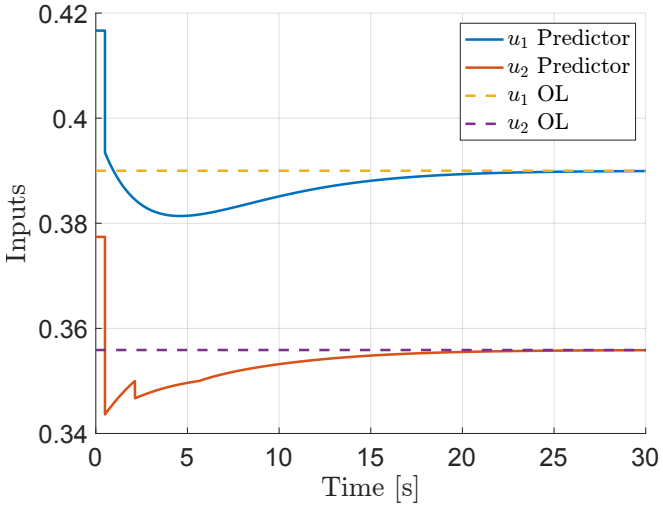

(b) Time-evolution of the flowrate ratios, for the proposed prediction-based control strategy and in open-loop.

Fig. 4: Simulation results obtained with f as pictured in Fig 3. A reference step is performed at $t = 1s$, while the system is originally at the equilibrium $y_1^0 = y_2^0 = 0.9$ with $u_1^0 = f^{-1}(y_1^0) \approx 0.42$ and $u_2^0 = f^{-1}\left(y_2^0/g(u_1^0)\right) \approx 0.38$. Feedback gains are picked as $k_1 = (1 - W(e^{-1})/(w_1^0 + T_{11}) \approx 0.71$ and $k_2 = 3$.

One can straighforwardly prove the following result, by studying the derivative of G.

Lemma 2: Consider G defined in (49). If $bk \geq 2$, G is monotonic (decreasing if $p > a$, increasing if $p < a$, constant if $p = a$). Otherwise, G admits an extremum at $h = 2 - bk$, which is $G(2 - bk) = a - e^{-2+bk}(p - a)$.

The following results can then be obtained.

Lemma 3: Consider G defined in (49) and denote

$$\kappa(a, p, b, k) \triangleq \sup_{y \in G(\mathbb{R}_+)} |y - a| \qquad (50)$$

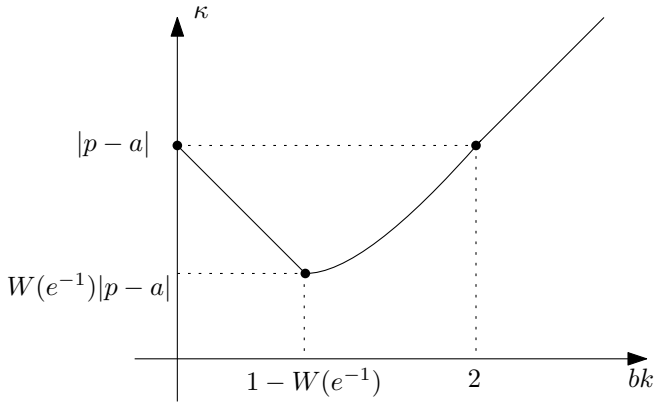

Fig. 5: Variations of κ defined in (50) with respect to bk for fixed values of a and p.

It holds

$$\kappa(a,p,b,k)=\begin{cases}(1-bk)|a-p| & \text{if } bk\leq 1-W(e^{-1})\\ e^{-2+bk}|a-p| & \text{if } 1-W(e^{-1})\leq bk\leq 2\\ (bk-1)|a-p| & \text{if } bk\geq 2\end{cases} \tag{51}$$

where W is the Lambert function.

The variations of κ are depicted in Fig. 5.

Lemma 4: Consider G defined in (49) and and a non-empty interval $[G_m,G_M]\subset\mathbb{R}$ such that $(p,a)\in[G_m,G_M]^2$. Then, $G(\mathbb{R}_+)\subset(G_m,G_M)$ iff

$$(1+e^2)a-e^2G_M\leq p\leq(1+e^2)a-e^2G_m \tag{52}$$

$$\text{and } k\in(0,k^\star(G_m,G_M,a,p,b)) \tag{53}$$

in which

$$k^\star(G_m,G_M,a,p,b) \tag{54}$$
$$=\frac{1}{b}\begin{cases}1+\xi(G_m,G_M,a,p) \text{ if } 2a-G_M\leq p\leq 2a-G_m\\ 2+\ln(\xi(G_m,G_M,a,p)) \text{ otherwise}\end{cases}$$

and

$$\xi(G_m,G_M,a,p)=\begin{cases}\dfrac{a-G_m}{p-a} & \text{if } p>a\\ \dfrac{G_M-a}{a-p} & \text{if } p<a\\ +\infty & \text{if } p=a\end{cases} \tag{55}$$

REFERENCES

[1] Z. Artstein. Linear systems with delayed controls: a reduction. *IEEE Transactions on Automatic Control*, 27(4):869–879, 1982.

[2] N. Bekiaris-Liberis, D. Bresch-Pietri, and N. Petit. Compensation of input-dependent hydraulic input delay for a model of a microfluidic process under zweifach–fung effect. *Automatica*, 160:111428, 2024.

[3] D. Bresch-Pietri, J. Chauvin, and N. Petit. Prediction-based stabilization of linear systems subject to input-dependent input delay of integral-type. *IEEE Transactions on Automatic Control*, 59(9):2385–2399, 2014.

[4] D. Bresch-Pietri and N. Petit. Implicit integral equations for modeling systems with a transport delay. *Recent results on time-delay systems: analysis and control*, pages 3–21, 2016.

[5] C.-H. Clerget and N. Petit. Optimal control of systems subject to input-dependent hydraulic delays. *IEEE Transactions on Automatic Control*, 66(1):245–260, 2020.

[6] Y. C. Fung and B. W. Zweifach. Microcirculation: mechanics of blood flow in capillaries. *Annual Review of Fluid Mechanics*, 3(1):189–210, 1971.

[7] M. Krstic. Delay compensation for nonlinear, adaptive, and pde systems. 2009.

[8] W. Kwon and A. Pearson. Feedback stabilization of linear systems with delayed control. *IEEE Transactions on Automatic Control*, 25(2):266–269, 1980.

[9] F. Mazenc and M. Malisoff. Stabilization and robustness analysis for time-varying systems with time-varying delays using a sequential subpredictors approach. *Automatica*, 82:118–127, 2017.

[10] F. Mazenc, S.-I. Niculescu, and M. Krstic. Lyapunov–krasovskii functionals and application to input delay compensation for linear time-invariant systems. *Automatica*, 48(7):1317–1323, 2012.

[11] F. Paratore, V. Bacheva, M. Bercovici, and G. Kaigala. Reconfigurable microfluidics. *Nature Reviews Chemistry*, 6(1):70–80, 2022.

[12] J. H. Perry. Chemical engineers' handbook, 1950.

[13] N. Petit. Control of microfluidic separation processes governed by the zweifach-fung effect. *Journal of Process Control*, 132:103124, 2023.

[14] A. Ponomarev. Nonlinear predictor feedback for input-affine systems with distributed input delays. *IEEE Transactions on Automatic Control*, 61(9):2591–2596, 2015.

[15] T. Strecker, O. M. Aamo, and M. Cantoni. Predictive feedback boundary control of semilinear and quasilinear 2×2 hyperbolic pde–ode systems. *Automatica*, 140:110272, 2022.

[16] P. Tabeling. *Introduction to microfluidics*. Oxford university press, 2005.

[17] X. Xu, L. Liu, M. Krstic, and G. Feng. Stability analysis and predictor feedback control for systems with unbounded delays. *Automatica*, 135:109958, 2022.

[18] S. Yang, A. Ündar, and J. D. Zahn. A microfluidic device for continuous, real time blood plasma separation. *Lab on a Chip*, 6(7):871–880, 2006.

[19] K. Zenger and A. J. Niemi. Modelling and control of a class of time-varying continuous flow processes. *Journal of Process Control*, 19(9):1511–1518, 2009.